Novel Covalently Cross-Linked Attapulgite/Poly(acrylic acid-co-acrylamide) Hybrid Hydrogels by Inverse Suspension Polymerization: Synthesis Optimization and Evaluation as Adsorbent...

ARTICLE *in* INDUSTRIAL & ENGINEERING CHEMISTRY RESEARCH · MARCH 2014

Impact Factor: 2.59 · DOI: 10.1021/ie4038054

4 AUTHORS, INCLUDING:

Peng Liu
Lanzhou University
242 PUBLICATIONS **3,924** CITATIONS
SEE PROFILE

Aiqin Wang
Chinese Academy of Sciences
296 PUBLICATIONS **6,281** CITATIONS
SEE PROFILE

I&EC research
Industrial & Engineering Chemistry Research

Article

pubs.acs.org/IECR

Novel Covalently Cross-Linked Attapulgite/Poly(acrylic acid-*co*-acrylamide) Hybrid Hydrogels by Inverse Suspension Polymerization: Synthesis Optimization and Evaluation as Adsorbents for Toxic Heavy Metals

Peng Liu,*[,†] Liping Jiang,[†,‡] Longxiang Zhu,[†] and Aiqin Wang[§]

[†]State Key Laboratory of Applied Organic Chemistry, Institute of Polymer Science and Engineering, College of Chemistry and Chemical Engineering, Lanzhou University, Lanzhou 730000, China

[‡]Department of Chemistry, Gansu Lianhe University, Lanzhou 730000, China

[§]Center of Xuyi Attapulgite Applied Technology, Lanzhou Institute of Chemical Physics, Chinese Academy of Science, Lanzhou 730000, China

Supporting Information

ABSTRACT: Novel covalently cross-linked microbeads of attapulgite/poly(acrylic acid-*co*-acrylamide) [ATP/P(AA−AM)] hybrid hydrogels with excellent mechanical stability were synthesized by the inverse suspension copolymerization of acrylic acid (AA) and acrylamide (AM) with multifunctional attapulgite nanorods (MF-ATP) as the sole cross-linker. The synthesis conditions, such as feeding method, neutralization degree of AA, and feed ratio of the comonomers to MF-ATP, were optimized scientifically. The TGA results showed that 96% of the comonomers (AA and AM) were grafted onto the MF-ATP nanorods to form a three-dimensional network skeleton of the hybrid hydrogels, for a feed ratio of MF-ATP nanorods to comonomers of 1:5. The ATP/P(AA−AM) hybrid hydrogels exhibited selective adsorption toward toxic heavy-metal ions, especially Pb^{2+} and Cu^{2+} ions. In addition, the adsorbed ions could be easily desorbed, indicating the reusability of the ATP/P(AA−AM) hybrid hydrogels. Their use as an adsorbent for toxic heavy-metal ions can therefore be expected to be economically and technically feasible.

1. INTRODUCTION

Toxic heavy metals cause a range of ailments and seriously threaten ecosystem and public health.[1] In the electroplating industry, the copper plating process is applied not only to form copper top coats on plating pieces, but also to obtain priming coats to improve interlayer adhesion before the plating of other metals such as nickel, silver, and chrome. Therefore, copper-containing wastewater is the most common waste in the electroplating industry. Although Cu is an essential trace mineral in the human body, excessive intake of copper can cause copper-poisoning symptoms, such as stomachache, diarrhea, and vomiting; some heavy patients suffer from gastrointestinal ulcers, liver and kidney damage, shock, or even death. Similarly, lead-containing wastewater usually comes from the electroplating, mining, and printing industries, as well as the manufacturing of batteries, paints, cosmetics, and so on. Lead poisoning is very dangerous, especially to children and pregnant women. Lead can lead to liver and kidney damage, mental retardation, anemia, muscular paralysis, and even death.

Adsorption of heavy-metal elements with various adsorbents, such as clays,[2] nanosized metal oxides,[3] polymer and polymer-based hybrids,[4] and agro-industrial and municipal waste materials,[5] has been of interest for water treatment. In recent years, adsorption has been one of the key areas of activity in wastewater treatment in the development of low-cost adsorbents with excellent adsorption efficiency, good mechanical stability, and simple operating performance.

Hybrid hydrogels have attracted intense interest for water treatment because of their excellent adsorption performances.[6] To date, many hybrid hydrogels have been prepared for the removal of inorganic ions[7−13] and organic pollutants[14−22] from water through in situ polymerization[7−12,14−20] or in situ formation.[21] In most hybrid hydrogel adsorbents, *N*,*N*′-methylenebisacrylamide,[7−12,14−16] glutaraldehyde,[13] polyethyleneglycol (400) diacrylate,[17] or 4,4′-bis(methacryloylamino)-azobenzene[21] has been used as the foreign organic cross-linker. In addition, clays have also been used as cross-linkers in hybrid hydrogel adsorbents through the hydrogen bonds between poly(acrylamide) and clays.[18−20]

Attapulgite (ATP) is an inexpensive clay mineral with a natural nanorod structure. However, unmodified ATP has a very high surface energy and readily agglomerates, which would substantially lower its adsorption efficiency. In addition, the difficult separation of ATP nanorods from solution obviously limits practical applications of ATP as an effective adsorbent.

In the present work, multifunctional attapulgite (MF-ATP) nanorods were synthesized by in situ surface modification with γ-methacryloxypropyltrimethoxysilane (KH-570) and used directly as the sole cross-linker for the formation of novel covalently cross-linked attapulgite/poly(acrylic acid-*co*-acryla-

Received: November 10, 2013
Revised: February 23, 2014
Accepted: February 25, 2014
Published: February 25, 2014

dx.doi.org/10.1021/ie4038054 | *Ind. Eng. Chem. Res.* 2014, 53, 4277−4285

mide) [ATP/P(AA−AM)] hybrid hydrogels through successive inverse suspension copolymerization of acrylic acid (AA) and acrylamide (AM) in liquid paraffin. The proposed in situ "one-pot" polymerization technique is a much simpler way to form the three-dimensional cross-linking network structure of hybrid hydrogels than the traditional preparation approaches, in which the clay nanomaterials are modified with polymerizable groups, separated, and finally dispersed in the polymerizing system.[22] It is also relative low-cost by eliminating the use of any foreign organic cross-linker. The ATP/P(AA−AM) hybrid hydrogels exhibited strong mechanical stability because of the reinforcement effect of the MF-ATP nanorods through the covalent cross-linking. More importantly, plenty of the carboxyl and amido groups enhanced and improved their adsorption capacity and adsorption selectivity toward the toxic heavy-metal ions, especially Pb^{2+} and Cu^{2+} ions.

2. EXPERIMENTAL METHODS

2.1. Materials. Attapulgite mineral was obtained from R&D Center of Xuyi Attapulgite Applied Technology, Lanzhou Institute of Chemical Physics, Chinese Academy of Sciences.

Acrylic acid (AA), acrylamide (AM), and ammonium persulfate (APS) were analytical reagents from Tianjin Kaixin Chemical Industry Co. Ltd., Tianjin, China. γ-Methacryloxypropyltrimethoxysilane (KH-570) was provided by Jiangsu Chenguang Silane Co., Ltd., Jiangsu, China. Span 80 and liquid paraffin were purchased from Tianjin Guangfu Fine Chemical Research Institute, Tianjin, China. Ammonium persulfate (APS), hydrochloric acid (HCl), and other reagents used were all analytical-reagent grade, obtained from Tianjin Chemicals Co. Ltd. (Tianjin, China) and used without further treatment. Distilled water was used throughout.

2.2. MF-ATP Nanorods. ATP mineral was dispersed in water until uniform in the nanorod state, acidified in 0.10 mol/L HCl to release more surface hydroxyl groups,[23] and filtered with an air pump to obtain an ATP aqueous dispersion with a solid content of 22 wt %.

MF-ATP nanorods were prepared as follows: Span 80 (0.5 g) and liquid paraffin (30 g) were placed in a Wolff bottle, and the mixture was stirred for 0.5 h. After 10 g of ATP dispersion had been added, the mixture was stirred for another 0.5 h. Then, 0.73 g of KH-570 was added, and the final mixture was stirred for 0.5 h, heated to 60 °C, and stirred for 6 h at this temperature. The MF-ATP dispersion was directly used in the subsequent in situ polymerization.

2.3. ATP/P(AA−AM) Hybrid Hydrogels. ATP/P(AA−AM) hybrid hydrogels were synthesized by different feeding techniques as detailed in the following subsections.

2.3.1. Pre-Emulsification Process. First, 5 g of AM was dissolved in the MF-ATP dispersion and stirred at 400 rpm for 1.5 h to obtain component I.

Separately, 5.0 g of AA and 30 g of liquid paraffin were emulsified in a 100 mL beaker with 0.5 g of Span 80 as the emulsifier. This mixture was stirred at room temperature for 1 h to obtain a pre-emulsion (component II).

Then, component I was poured into component II, and the mixture was stirred for 0.5 h. After 0.10 g of APS had been added and the mixture had been stirred for 0.5 h, the mixture was stirred at 60 °C for 2 h and then at 80 °C for 3 h in a N_2 atmosphere.

AA (5.0 g) was added dropwise to 8.0 g of a 25% NaOH solution under stirring to obtain AA with a 70% neutralization degree. AA with a 50% neutralization degree was prepared similarly.

The samples of neutralized AA were also used for in situ polymerization according to the pre-emulsification process described above.

2.3.2. Continuous Drop Feeding. Span 80 (0.70 g) was added to liquid paraffin (42 g) and stirred for 0.5 h. Separately, 5.0 g of AM was dissolved in 4.0 g of water containing 5.0 g of AA and 0.10 g of APS, and this mixture was stirred for 0.5 h. Then, this mixture was added to the prepared Span 80-containing liquid paraffin and emulsified for 1 h. Finally, the MF-ATP dispersion was slowly added dropwise to this emulsion. The mixture was stirred at 60 °C for 2 h and at 80 °C for 3 h in a N_2 atmosphere.

The samples of neutralized AA were similarly used for in situ polymerization according to the continuous drop-feeding process.

2.3.3. Semicontinuous Drop Feeding. Span 80 (0.70 g) was added to 42 g of liquid paraffin and stirred for 0.5 h. Separately, 5.0 g of AM was dissolved in 4.0 g of water containing 5.0 g of AA and 0.10 g of APS, and this mixture was stirred for 0.5 h. Then, this mixture was added to the prepared Span 80-containing liquid paraffin and emulsified for 1 h. One-third of this emulsion was added to the MF-ATP dispersion, and the resulting mixture was stirred for 0.5 h. After the mixture had been heated to 60 °C, the remaining two-thirds of the emulsion was added dropwise within 1 h. Finally, the mixture was kept at 60 °C for 2 h and at 80 °C for 3 h in a N_2 atmosphere.

The samples of neutralized AA were similarly used for in situ polymerization according to the semicontinuous drop-feeding process.

2.3.4. Single-Factor Experiments on the Ratio of Monomers to MF-ATP. MF-ATP nanorods were prepared under the following conditions: the dosage of Span 80 was 5.0% of water, KH-570 was one-third of the mass of the ATP nanorods, and the ratio of the oil phase to the water phase (oil/water ratio) was 3:1.

A series of single-factor experiments were carried out to investigate the effect of the mass ratio of the total amount of comonomers (AA and AM) to the amount of ATP nanorods on the properties of the ATP/P(AA−AM) hybrid hydrogel. In these experiments, the ratio of monomers (AA + AM) to ATP was changed from 1:1 to 10:1, and the sample series was correspondingly numbered from 1 to 10. In addition, the other conditions were kept unchanged: the dosage of Span 80 was 5% of the amount of water, the oil/water ratio was 3:1, and APS was 1.0 wt % of the total amount of AA and AM.

2.4. Post-Treatments of ATP/P(AA−AM) Hybrid Hydrogels. The ATP/P(AA−AM) hybrid hydrogels were separated from liquid paraffin and washed with ether, ethanol, and water in sequence. Then, possible ungrafted copolymers were removed by immersing the products in an ammonia/water mixture at pH 8−9 for 24 h and extracting them in water for 24 h; this process was repeated three times. The final ATP/P(AA−AM) hybrid hydrogels were partially dried at 80 °C and then thoroughly dried in a vacuum oven at 70 °C.

2.5. Adsorption and Desorption. *2.5.1. Preliminary Research with Cu^{2+}.* An accurately weighed sample of about 0.1 g of the ATP/P(AA−AM) hybrid hydrogels was added to 50 mL of a 100 mg/L Cu^{2+} solution at pH 5.12. After the mixture had been stirred for 3 h, the specimen was removed and further diluted with pH 1.0 aqueous HCl to a given concentration that avoided the hydrolysis of the ion. The

dx.doi.org/10.1021/ie4038054 | Ind. Eng. Chem. Res. 2014, 53, 4277−4285

original and remaining Cu^{2+} concentrations were measured by flame atomic absorption spectrometry (FAAS, AA 240 atomic absorption spectrometer, Varian, Palo Alto, CA) to evaluate the adsorption capacity toward Cu^{2+} ion. For all of the FAAS determinations, the data are presented as averages of three measurements with relative standard deviations of less than 5%.

After the Cu^{2+}-adsorbed ATP/P(AA−AM) hybrid hydrogels had been filtered, washed with distilled water, and wiped with filter paper to remove solution remaining on the surface, they were put into 50 mL of a 1.0 mol/L aqueous solution of HCl and stirred for 1 h. The Cu^{2+} ion concentration in the upper liquid was measured by FAAS to evaluate the elution ratio.

The adsorption capacity of the sample toward the metal ion (q_e) was calculated as

$$q_e = 0.05(C_0 - C_e)/W \quad (1)$$

where W represents the mass of dried ATP/P(AA−AM) hybrid hydrogels sample, and C_e represents the concentration of the metal ion remaining after adsorption, as measured by FAAS.

2.5.2. Adsorption Selectivity of ATP/P(AA−AM) toward Heavy-Metal Ions. An accurately weighed sample of about 0.1 g of the ATP/P(AA−AM) hybrid hydrogels was added to 50 mL of a mixed solution containing the same concentration (100 mg/L) of five heavy-metal ions (Pb^{2+}, Zn^{2+}, Cd^{2+}, Cu^{2+}, and Ni^{2+}) and stirred for 3 h. The original and remaining concentrations of each ion were measured to evaluate the corresponding adsorption capacity and adsorption selectivity.

2.5.3. Adsorption and Desorption of Pb^{2+} or Cu^{2+} Ions. The effects of the adsorption-medium pH and adsorption time on the adsorption capacities of ATP/P(AA−AM) samples were studied by stirring the samples (about 0.1 g, accurately weighed) in 50 mL of 100 mg/L Pb^{2+} or Cu^{2+} solutions at different pH values (1, 2, 3, 4, 5, and 6) for certain lengths of time (1, 2, 2.5, 3, 3.5, 4, 5, 7, 9, and 16 h). The remaining Pb^{2+} or Cu^{2+} concentrations were measured to calculate the adsorption capacities toward Pb^{2+} or Cu^{2+}.

After adsorption had been saturated under optimized conditions, the heavy-metal-ion-adsorbed ATP/P(AA−AM) samples were separated and stirred in an aqueous HCl solution. The concentrations of desorbed heavy-metal ions were measured by FAAS to investigate the desorption ratio.

2.6. Adsorption Isotherms. An accurately weighed sample of about 0.1 g of the ATP/P(AA−AM) hybrid hydrogels (sample 5) was added to 50 mL of a solution containing Pb^{2+} or Cu^{2+} at a concentration of 20, 40, 60, 80, or 100 mg/L at pH 5.0. Each resulting mixture was stirred at 293, 303, or 313 K for 9 h. The remaining concentrations of the heavy-metal ions (C_e) in each of the specimen were measure by FAAS to calculate q_e according to eq 1.

2.7. Characterization. *2.7.1. Physical Parameters.* The reaction was primarily evaluated by investigating the physical parameters, such as the sedimentation velocity immediately after stirring was stopped, the size homogeneity of the ATP/P(AA−AM) hybrid hydrogels and the clarity of liquid paraffin.

2.7.2. Swelling Capacity (C_s). The dried ATP/P(AA−AM) hybrid hydrogels were weighed and immersed in distilled water for 24 h. The swelling capacity (C_s) was measured as the mass ratio of water absorbed to dried ATP/P(AA−AM) hybrid hydrogels. The data are presented as averages of three measurements with relative standard deviations of less than 5%.

2.7.3. Mechanical Stability. The resistance to shear flow of the ATP/P(AA−AM) hybrid hydrogels was studied by immersing them in water for 24 h and then stirring the hyrogel-containing water at 5000 rpm for 2 h. The damage rates of the swelled ATP/P(AA−AM) hybrid hydrogels were investigated to evaluate their ability to resist shearing.

The pressure resistance was evaluated by placing a given weight on the swollen hybrid hydrogels. The load-bearing ability of the swelled ATP/P(AA−AM) hybrid hydrogels was used to estimate their pressure-resistance stability.

2.7.4. FT-IR Spectroscopy. Bare ATP, MF-ATP, and ATP/P(AA−AM) hybrid hydrogels were characterized wit an h Avatar 360 FT-IR spectrometer (Nicolet, Madison, WI) in the range of 400−4000 cm^{-1} at a resolution of 4 cm^{-1} with the KBr pellet method.

2.7.5. Thermogravimetric Analysis (TGA). A thermogravimetric analyzer (TGA 2050, TA Instruments, New Castle, DE) was used to evaluate the amount of organic molecules grafted on the ATP surface, at a heating rate of 20 °C/min in a N_2 atmosphere to avoid oxidation during the TGA process.

3. RESULTS AND DISCUSSION

3.1. Preparation Conditions. *3.1.1. Feeding Process.* In the continuous and semicontinuous drop-feeding processes, the products appeared to be a uniform, viscous, and sticky sol; no hydrogel-like products were obtained (Figure S1, Supporting Information). This might be because the concentration of Span 80 was much higher and those of monomers and APS were much lower at the beginning of the reaction, compared with the pre-emulsion process, so that the polymerization stayed in the "starved state" all the time and consequently formed many more primary nuclei in the continuous or semicontinuous drop-feeding processes.[24] Alternatively, it might be difficult to form the desired hybrid hydrogels with a certain radius; that is, these processes tend to produce latex particles.[25] Finally, the products were in the form of suspended powders or viscous emulsions. Therefore, the pre-emulsion process was selected for further analysis.

3.1.2. Neutralization Degree of AA. In the polymerizations by the pre-emulsification process using neutralized AA as the comonomer, hydrogel-like products were observed. However, the products were suspended in liquid paraffin for a long time (Figure S2, Supporting Information), whereas the hydrogel-like products settled rapidly once the stirring was stopped only in the polymerization using non-neutralized AA as the comonomer (Figure S3, Supporting Information).

An increase of the neutralization degree of AA results in the growth in number of electronegative carboxyl groups inside the polymer. Swelling occurs when intraparticle ionic repulsion and osmotic forces exceed attractive forces.[26] Ionized carboxyl groups repel with each other, leading to the expansion of the hydrogels, which, in turn, decreases the density of the hydrogels. In addition, hydrogen bonding is a key issue in the aggregation process of molecules in water.[27] An increase in the number of carboxyl groups results in an increase in the number of hydrogen bonds between the carboxyl groups and water molecules, and the formed hydrogen-bond network structure is more stable.[28] Hydrogen bonds show a certain directional property, which leads to the orientation of the carboxyl groups and water molecules, producing an anisotropic hydrogel network[29] and restricting the motion of the polymer segments. As a result, the distances among chain segments increase, which also decreases the density of the hydrogels. Another possibility is the swelling of the preneutralized PAA chains or segments during the polymerization process.[30] As a result, the hydrogels synthesized with neutralized AA tend to be

dx.doi.org/10.1021/ie4038054 | Ind. Eng. Chem. Res. 2014, 53, 4277−4285

suspended in the liquid paraffin and do not settle within a short period. This would certainly go against treatment of the products, such as separation. Based on these preliminary experiments, polymerization with neutralized AA as the comonomer was ruled out for further single-factor experiments.

3.1.3. Feed Ratio of Comonomers to MF-ATP. A series of single-factor experiments was designed to investigate the effects on the products of the feed ratio between the comonomers (AM and AA) and the MF-ATP nanorods. It was found that the products from formulas 1−4 [with mass ratios of MF-ATP nanorods to comonomers of MF-ATP/(AA + AM) = 1:1−1:4] appeared to be uniform, viscous, and sticky sols, whereas those from formulas 5−10 [with MF-ATP/(AA + AM) = 1:5−1:10] produced hybrid hydrogels. All of the obtained hybrid hydrogels sedimented from liquid paraffin immediately after stirring was stopped. It can thus be concluded that hybrid hydrogels can be obtained only when the MF-ATP/(AA + AM) feed ratio is equal to or less than 1:5 (Figure S4, Supporting Information).

3.2. Swelling Capacity (C_s). The hybrid hydrogels appeared to obviously swell in water (Figure S5, Supporting Information), so their C_s values were calculated,[31] as summarized in Table 1. From Table 1, one can see that the

Table 1. Swelling Capacities (C_s, %) and Utilizations of the Comonomers (UC, %) of Hybrid Hydrogels from Formulas 5−10

no.	MF-ATP/(AA + AM)[a]	C_s[b] (%)	UC[c] (%)
5	1:5	263	96.0
6	1:6	255	87.7
7	1:7	197	89.2
8	1:8	219	85.1
9	1:9	265	90.0
10	1:10	257	94.3

[a]MF-ATP/(AA + AM) is the mass ratio of MF-ATP nanorods to comonomers (AA + AM), in which the mass ratio of AA to AM is 1:1. [b]Tested after being immersed in distilled water for 24 h. [c]Calculated from TGA results.

C_s values of samples 7 and 8 were very low. Those of samples 6 and 10 were significantly higher but still slightly lower than those of samples 5 and 9. The likely reason for these differences is that the hybrid hydrogels of samples 7 and 8 showed certain aggregation, those of samples 6 and 10 underwent only slight aggregation, and those of samples 5 and 9 exhibited no aggregation, as observed from Figure S4 (Supporting Information). Furthermore, the C_s values of samples 5 and 9 and of samples 6 and 10 were similar, indicating that the dosage of AA and AM had a minor effect on the cross-linking density of the hybrid hydrogels.

3.3. Mechanical Stability. None of the ATP/P(AA−AM) hybrid hydrogels was broken after being stirred at 5000 rpm for 2 h (Figure S6, Supporting Information) or showed any cracks under a 3-kg load (Figure S7, Supporting Information). These results verified that the ATP nanorods significantly reinforced the mechanical properties of the hybrid hydrogels. The covalent linking between the copolymer matrix [poly(acrylic acid-*co*-acrylamide), P(AA−AM)] and the ATP nanorods increased the flexural moduli and restricted the segmental motion of the ATP/P(AA−AM) network,[32] which further improved the mechanical and dimensional stability.[33−35] These are the key performance metrics for improving the application stability and reproducibility of ATP/P(AA−AM) hybrid hydrogels and reducing their cost.

3.4. Utilization of Comonomers. The utilization of the comonomers (UC, %), namely, the ratio of the measured copolymer content (CC, %) to the theoretical value (feed ratio), is another important factor affecting the cost of hybrid hydrogels. TGA was used to investigate the organic content in MF-ATP and the copolymer content (CC, %), namely, the ratio between the weight of copolymer grafted and the weight of the hybrid hydrogels, in the ATP/P(AA−AM) hybrid hydrogels (Figure 1). The analysis revealed that the organic

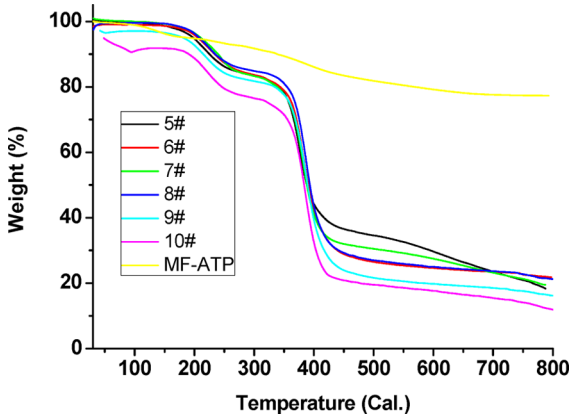

Figure 1. TGA curves of MF-ATP nanorods and hybrid hydrogel samples 5−10.

content in the MF-ATP nanorods was 17.8%. Compared to the theoretical value of 25%, it can be concluded that only a small portion of KH-570 hydrolyzed and self-polymerized.

The weight losses in the temperature range of 150−450 °C were ascribed to the thermal decomposition of the organic compounds [KH-570 and copolymer P(AA−AM)] and were found to be 81.4%, 77.9%, 80.4%, 78.7%, 83.2%, and 87.0% for samples 5−10, respectively. The CC values of ATP/P(AA−AM) hybrid hydrogels samples 5−10 were subsequently calculated to be 77.0%, 72.7%, 75.8%, 73.7%, 79.2%, and 83.9%, respectively. The UC values of samples 5−10 were also calculated and are presented in Table 1. One can see that the UC values of samples 5−10 were in the range of 85.1−96.0% and sample 5 exhibited the highest value. That is, almost all of the comonomers were grafted onto the ATP nanorods in sample 5. Moreover, the feed ratio of the MF-ATP nanorods to the comonomers in formula 5 was the highest, indicating the lowest cost of sample 5 in the series.

3.5. FT-IR Analysis. The FT-IR spectra of bare ATP, MF-ATP nanorods, and ATP/P(AA−AM) hybrid hydrogel sample 5 are compared in Figure 2. An absorbance peak of methyl groups around 2900 cm^{-1}, which does not exist in the spectrum of bare ATP nanorods, appears in the spectrum of MF-ATP nanorods, suggesting that KH-570 was successfully grafted onto the ATP nanorods. Two absorbance peaks around 2800 and 2900 cm^{-1} can be observed in the spectrum of the ATP/P(AA−AM) hybrid hydrogels. These two peaks are more obvious than in the spectrum of MF-ATP nanorods, indicating that the copolymer (AA−AM) was successfully grafted onto the ATP nanorods through copolymerization with the polymerizable groups on the surfaces of the MF-ATP nanorods. In addition, a weak peak appears around 1690 cm^{-1} (in-plane

dx.doi.org/10.1021/ie4038054 | Ind. Eng. Chem. Res. 2014, 53, 4277−4285

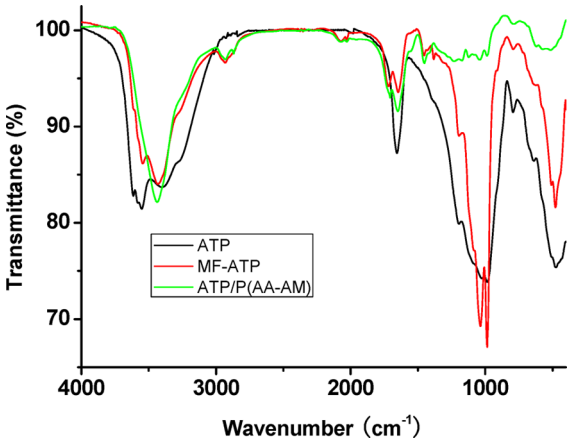

Figure 2. FT-IR spectra of bare ATP, MF-ATP nanorods, and ATP/P(AA−AM) hybrid hydrogel (sample 5).

deformation vibration of amido group), suggesting that AM was also grafted onto the ATP nanorods.

3.6. Adsorption Performance. *3.6.1. Adsorption Capacity toward Cu^{2+} Ion and Desorption Ratio.* The adsorption properties of the ATP/P(AA−AM) hybrid hydrogels (samples 5−10) were preliminarily tested with Cu^{2+} ion. Their adsorption capacities and the corresponding desorption ratios with 1.0 mol/L HCl aqueous solution are presented in Figure 3. The results reveal that the adsorption capacities of

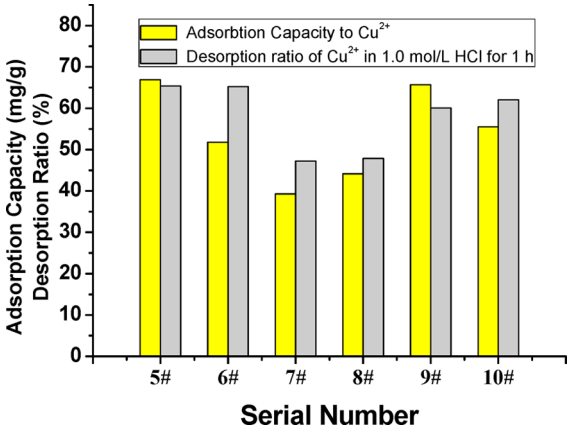

Figure 3. Adsorption capacities of ATP/P(AA−AM) hybrid hydrogels for Cu^{2+} ion and corresponding desorption ratios in 1.0 mol/L HCl aqueous solution.

samples 7 and 8 toward Cu^{2+} ion were very low. This is because their diameters increased as a result of aggregation and the surface adsorption increased. The adsorbed metal ions on the surface acted as metallic-ion cross-linking agents. The metallic-ion cross-linking resulted in elastic shrinkage of the polymer chains. As a result, further permeation of heavy-metal ions was hampered. On the other hand, the electrostatic repulsion between the metal ions on the surface and those in solution also has a negative impact on the further adsorption of heavy-metal ions.[36]

Samples 6 and 10 exhibited adsorption capacities higher than those of samples 7 and 8 but lower than those of samples 5 and 9 because of their slight aggregation. This indicates that aggregation among the ATP/P(AA−AM) hybrid hydrogels has an obviously negative effect on the adsorption capacity, consistent with the results for C_s. The adsorption capacities of samples 5 and 9 toward Cu^{2+} ion reached 66.93 and 65.70 mg/g, respectively, and their desorption ratios with 1.0 mol/L HCl solution in only 1 h reached 65.41% and 60.04%, respectively, also higher than those of other samples. Therefore, samples 5 and 9 are the preferred ones.

3.6.2. Adsorption Selectivity of ATP/P(AA−AM) toward Heavy-Metal Ions. The competitive adsorptions of the ATP/P(AA−AM) hybrid hydrogels toward five heavy-metal ions (Pb^{2+}, Zn^{2+}, Cd^{2+}, Cu^{2+}, and Ni^{2+}) are compared in Figure 4.

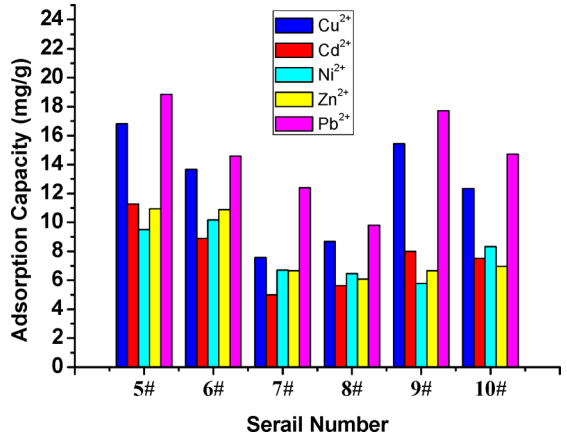

Figure 4. Adsorption capacities of ATP/P(AA−AM) hybrid hydrogels for different heavy-metal ions.

All five samples showed good adsorption selectivities toward Cu^{2+} and Pb^{2+} ions, and sample 5 (16.8% of Cu^{2+} and 18.9% of Pb^{2+}) and sample 9 (15.5% of Cu^{2+} and 17.7% of Pb^{2+}) showed higher adsorption capacities than the others, similarly to Figure 3. The better adsorption selectivity of the hybrid hydrogels might result from their adsorption mechanism: both ion-exchanging and chelating. These results further verify that aggregation among the ATP/P(AA−AM) hybrid hydrogels has obviously negative effects on their adsorption capacities toward heavy-metal ions. Therefore, the adsorption properties of samples 5 and 9 toward Cu^{2+} and Pb^{2+} ions were studied further.

3.6.3. Effects of Adsorption-Medium pH on Adsorption Capacity toward Pb^{2+}or Cu^{2+} for Samples 5 and 9. As shown in Figure 5, the adsorption capacity of sample 5 toward Pb^{2+} ion was near zero for pH < 1; it increased sharply from pH 2 to 3, then reached a plateau from pH 3 to 4, and increased again from pH 4 to 6. Similar changes were observed for sample 9. The only difference is that the increase in adsorption capacity of sample 9 toward Pb^{2+} ion from pH 4 to 6 was much faster. This resulted from the complex anions. In the lower-pH HCl solution, Pb^{2+} ion can complex with Cl^- ion to form complex anions, such as $PbCl_4^{2-}$ and $PbCl_3^-$, whose concentrations decrease with increasing pH; that is, the concentration of free Pb^{2+} increases with increasing pH. These results can be ascribed to the following reasons: At low pH, on one hamd, more hydrogen ions compete with Pb(II) for adsorption sites, which makes the accessibility of Pb(II) to activated sites difficult; on the other hand, carboxyl groups in the adsorbents exist in the form of −COOH rather than $-COO^-$, which could go against the possibility of Pb(II) adsorbing onto the adsorbents.[37] To avoid the occurrence of precipitation in the aqueous solution, a

dx.doi.org/10.1021/ie4038054 | Ind. Eng. Chem. Res. 2014, 53, 4277−4285

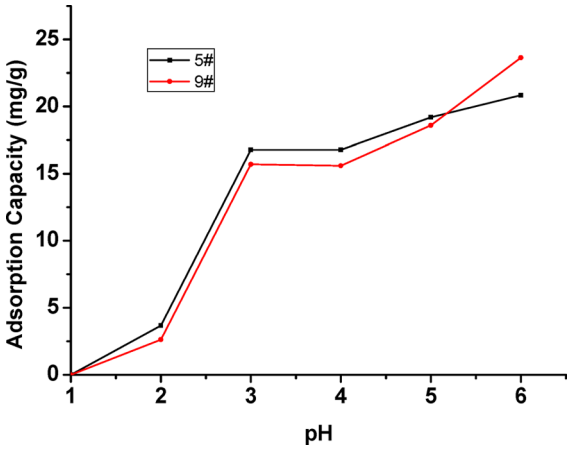

Figure 5. Adsorption capacities of ATP/P(AA−AM) hybrid hydrogels (samples 5 and 9) for Pb^{2+} ion at different pH values for 3 h.

pH value of 5 was selected as the initial pH value of Pb(II) solution for subsequent adsorption experiments.

There was only one abrupt change in the pH range of 2−4 for Cu^{2+}, and the adsorption capacity reached a plateau from pH 4 to 6 (Figure 6), possibly because the pK_a value of the

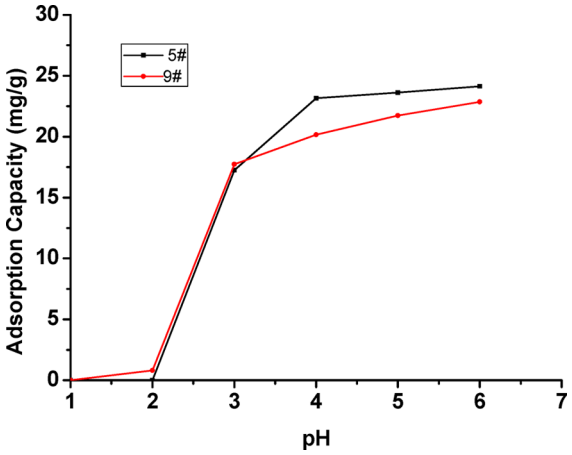

Figure 6. Adsorption capacities of ATP/P(AA−AM) hybrid hydrogels (samples 5 and 9) for Cu^{2+} ion at different pH values for 3 h.

carboxyl group is about 4.0.[38] To achieve relatively higher adsorption capacities toward Pb^{2+} or Cu^{2+} ions and simultaneously avoid the hydrolysis of Pb^{2+} or Cu^{2+} ions, the pH value the aqueous HCl should be set at 5.0.

In addition, the results from Figures 5 and 6 show that the adsorption capacities of sample 5 toward both Pb^{2+} and Cu^{2+} ions were slightly higher than those of sample 9 in pH 5.0 HCl medium; meanwhile, the dosage of AA and AM in sample 9 was higher than that in sample 5. Therefore, sample 5 was selected for further experiments by considering the adsorption capacities toward Pb^{2+} or Cu^{2+} ions and the adsorbent cost.

3.6.4. Adsorption Equilibrium Time of Sample 5 toward Pb^{2+} or Cu^{2+}. The rate of adsorption of Pb^{2+} ion on sample 5 was very high in the first 3 h (Figure 7), indicating that Pb^{2+} permeated into the outer surface of the ATP/P(AA−AM) hybrid hydrogel through film diffusion. This was followed by a plateau between 3 and 4 h due to the saturation of Pb^{2+} on the outer surface of the sample and the decrease of film diffusion; then a rapid increase again from 4 to 9 h, implying that the

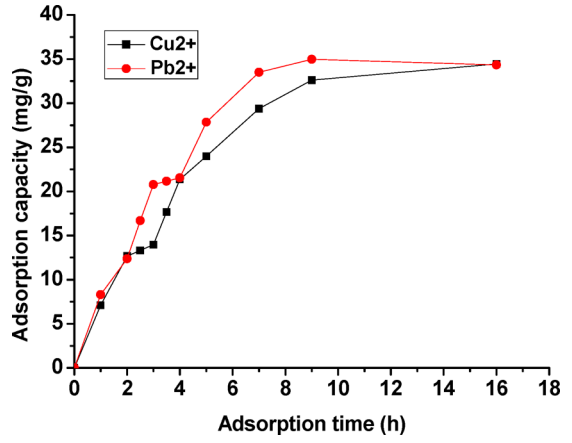

Figure 7. Adsorption capacities of sample 5 toward Pb^{2+} and Cu^{2+} ions as functions of adsorption time.

migration of Pb^{2+} ion was driven by film diffusion together with intraparticle diffusion; and finally another plateau from 9 to 16 h, suggesting that the adsorption reached saturation in about 9 h because of the slowing of both diffusion mechanisms.[39] The equilibrium adsorption capacity was calculated to be 34.98 mg of Pb^{2+} per gram of sample 5 in pH 5.0 HCl aqueous solution.

Compared to the adsorption of Pb^{2+}, a similar trend was observed for Cu^{2+}. The differences were that the first plateau appeared from 2 to 4 h, indicating that film diffusion slowed at 2 h and Cu^{2+} began to migrate into the inner part of the sample from 4 h; and the adsorption reached saturation in about 9 h, implying that the adsorption of Cu^{2+} onto ATP/P(AA−AM) hybrid hydrogel sample 5 reached equilibrium as rapidly as Pb^{2+} ion in pH 5.0 HCl aqueous solution. The equilibrium adsorption capacity was calculated to be 32.60 mg of Cu^{2+} per gram of sample 5 in pH 5.0 HCl aqueous solution.

3.7. Desorption of Adsorbed Metal Ions from Hybrid Hydrogel Sample 5. *3.7.1. Effect of HCl Concentration on the Desorption Ratio of Pb^{2+} or Cu^{2+}.* The desorption ratios (mass ratio of eluted ions to adsorbed ions) as a function of the aqueous HCl concentration are shown in Figure 8. It was found that 98.36% of adsorbed Pb^{2+} and 98.52% of adsorbed Cu^{2+} could be desorbed with 0.20 mol/L HCl aqueous solution in 2 h. At higher concentrations of HCl, Pb^{2+} reacts with the Cl^- to

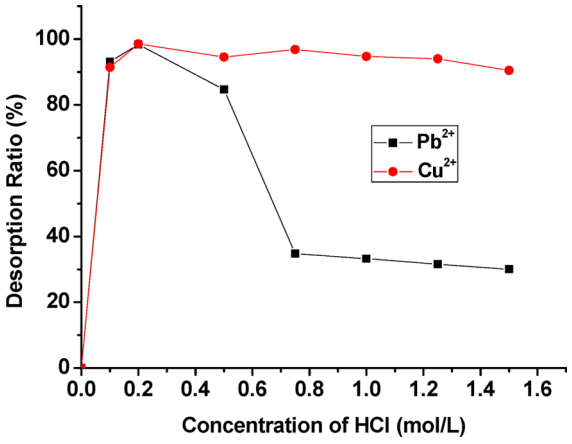

Figure 8. Desorption ratios of adsorbed Pb^{2+} and Cu^{2+} ions from saturated adsorbed sample 5 at different concentrations of HCl aqueous solution.

dx.doi.org/10.1021/ie4038054 | Ind. Eng. Chem. Res. 2014, 53, 4277−4285

form water-insoluble complexes that adsorb on the surface of the adsorbent. Consequently, the desorption ratio of Pb^{2+} showed a sharp decrease.

3.7.2. Effect of Time on the Desorption Ratio of Pb^{2+} or Cu^{2+} with 0.20 mol/L HCl. The desorption ratios of Pb^{2+} and Cu^{2+} as functions of time are shown in Figure 9. The

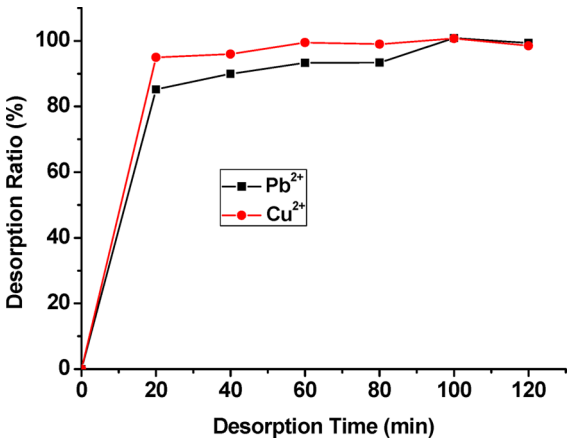

Figure 9. Desorption ratios of adsorbed Pb^{2+} and Cu^{2+} ions from saturated adsorbed sample 5 as functions of time in 0.20 mol/L HCl aqueous solution.

desorptions of Pb^{2+} and Cu^{2+} from sample 5 in 0.20 mol/L HCl reached equilibrium within 100 min, and both desorption ratios were as high as 100%, indicating that the adsorbed Pb^{2+} and Cu^{2+} could be desorbed from ATP/P(AA−AM) hybrid hydrogel sample 5 with 0.20 mol/L HCl within 100 min. These results reveal the excellent renewability of ATP/P(AA−AM) hybrid hydrogel adsorbents.

3.8. Adsorption Kinetics. Batch kinetic studies were carried out using an accurately weighed 0.10-g portion of ATP/P(AA−AM) hybrid hydrogel sample 5 in 50 mL of a solution of 100 mg/L Pb^{2+} or Cu^{2+} ion. After the solution had been stirred for 16 h, the remaining metal-ion concentration was determined. The obtained experimental data were analyzed with pseudo-first-order, pseudo-second-order, and intraparticle diffusion models as follows:[40]

The pseudo-first-order equation is given by

$$1/q_t = k_1/(q_e t) + 1/q_e \quad (2)$$

where k_1 (h^{-1}) is the pseudo-first-order adsorption rate constant, q_t (mmol/g) is the amount adsorbed at time t (h), and q_e (mmol/g) denotes the amount adsorbed at equilibrium.

The pseudo-second-order equation can be expressed as

$$t/q_t = 1/(k_2 q_e^{\,2}) + t/q_e \quad (3)$$

where k_2 [g/(mmol/h)] is the pseudo-second-order adsorption rate constant.

The linear form of the intraparticle diffusion equation is given by

$$\ln q_t = \ln k_i + \frac{1}{2}\ln t \quad (4)$$

where k_i [mmol/(g $h^{1/2}$)] is the intraparticle diffusion rate constant.

The kinetic parameters for adsorption of Pb^{2+} and Cu^{2+} by ATP/P(AA−AM) hybrid hydrogel sample 5 are summarized in Table 2. Based on Table 2, the R^2 values for the pseudo-second-order kinetic models of Pb^{2+} and Cu^{2+} (Figure S8b, Supporting Information) were near those for the pseudo-first-order kinetic models (Figure S8a, Supporting Information). However, the calculated equilibrium adsorption capacity values, $q_{e,cal}$, were also closer to the experimental $q_{e,exp}$ values. Therefore, it is reasonable to conclude that the rate-limiting step during the adsorption of Pb^{2+} and Cu^{2+} ions onto ATP/P(AA−AM) hybrid hydrogel sample 5 was chemisorption, involving valence forces through the sharing or exchange of electrons between the metal ion and the adsorbent.[41]

Table 2. Kinetic Parameters for the Adsorption of Pb^{2+} and Cu^{2+} onto ATP/P(AA−AM) Hybrid Hydrogel Sample 5

parameter	Pb^{2+}	Cu^{2+}
$q_{e,exp}$ (mmol/g)	0.1659	0.5425
Pseudo-First-Order Model		
k_1 (h^{-1})	5.726	6.177
$q_{e,cal}$ (mmol/g)	0.2643	0.7873
R^2	0.9753	0.9801
Pseudo-Second-Order Model		
k_2 [g/(mmol h)]	1.289	0.2291
$q_{e,cal}$ (mmol/g)	0.2147	0.7686
R^2	0.9646	0.9711
Intraparticle Kinetic Model[a]		
K_i (mmol/(g $h^{1/2}$))	0.0393, 0.1585	0.1103, 0.3365
R^2	0.9707, 0.1363	0.9678, 0.8500

[a]Values listed for $t < 7$ and $t > 7$, respectively.

The intraparticle diffusion plots showed multilinearity correlations, indicating that two steps occurred during the adsorption process (Figure S8c, Supporting Information). The first initial linear portion was followed by a plateau. The initial linear portion is deemed to be external surface adsorption. The second portion indicates a gradual adsorption stage in which intraparticle diffusion is rate-determining.[42]

3.9. Adsorption Isotherms. Adsorption isotherms were determined to establish the model of adsorption and reveal the adsorption characteristics at a constant temperature. In this study, the Langmuir and Freundlich isotherm equations were used to evaluate the adsorption isotherms of the ATP/P(AA−AM) hybrid hydrogels toward Pb^{2+} and Cu^{2+} ions.

The Langmuir isotherm equation assumes that the adsorption sites are distributed uniformly on the whole surface of the adsorbent and that only one adsorbate molecule is adsorbed onto each adsorption site.[43] Therefore, the Langmuir model is often used to evaluate monolayer adsorption at the interface between solid and liquid phases in dilute solutions. The linear Langmuir isotherm equation is expressed as

$$C_e/q_e = 1/(k_L q_L) + C_e/q_L \quad (5)$$

where q_e and C_e represent the concentrations of metal ions in the solid and liquid phases, respectively, at equilibrium and q_L and k_L represent the monolayer adsorption capacity and equilibrium constant for the adsorption, respectively.

The Freundlich isotherm equation is an empirical equation and describes adsorption on heterogeneous surfaces.[44] The linear Freundlich isotherm equation is expressed as

$$\ln q_e = \ln k_F + \frac{1}{n_F}\ln C_e \quad (6)$$

dx.doi.org/10.1021/ie4038054 | Ind. Eng. Chem. Res. 2014, 53, 4277−4285

where q_e and C_e represent the concentrations of metal ions in the solid and liquid phases, respectively, at equilibrium and k_F and n_F are constants.

Linear plots of the specific adsorption (C_e/q_e) against the equilibrium concentration (C_e) of Pb^{2+} and Cu^{2+} are shown in Figure S9 (Supporting Information). The Langmuir constants q_L and k_L of Pb^{2+} and Cu^{2+} were determined from the slopes and intercepts of the plots. The Freundlich isotherm data in terms of ln C_e and ln q_e were calculated based on the above-obtained values of C_e and q_e of sample 5 toward Pb^{2+} and Cu^{2+} at 293, 303, and 313 K. Linear plots of the Freundlich isotherm for Pb^{2+} and Cu^{2+} adsorption on sample 5 are shown in Figure S10 (Supporting Information). The Freundlich constants k_F and n_F were calculated from the intercepts and slopes of the plots.

The results of the adsorption isotherms indicate that the R_L^2 and R_F^2 values of all plots were higher than 0.95, implying that the adsorptions of Pb^{2+} and Cu^{2+} on sample 5 can be evaluated by both the Langmuir and Freundlich models. However, R_F^2 is closer to 1 than R_L^2 is, indicating that the adsorption at the interface between the solid and liquid phases were not as homogeneous as assumed in the Langmuir model; that is, the Freundlich isotherm is more suitable for expressing the adsorption of Pb^{2+} and Cu^{2+} on the surface of sample 5.

The results from the Langmuir isotherms reveal that the maximum capacities of monolayer adsorption of Pb^{2+} on the surface of sample 5 were 84.03, 138.89, and 158.73 mg/g at 293, 303, and 313 K, respectively, and the maximum capacities of monolayer adsorption of Cu^{2+} on the surface of sample 5 were 156.25, 208.33, and 256.41 mg/g at 293, 303, and 313 K, respectively. These data indicate that the saturated adsorption capacities of sample 5 for Pb^{2+} and Cu^{2+} increased with the temperature. The results also reveal that the adsorption capacities of sample 5 for Cu^{2+} and Pb^{2+} increased with increasing initial concentrations of metal ions at a constant temperature and finally reached the maximum finally. This was because the osmotic pressure increased with increasing initial concentration of Cu^{2+} and Pb^{2+}, and the P(AA−AM) chain segments among the ATP nanorods showed certain elastic stretch under the osmotic pressure. As a result, the grid size of the ATP/P(AA−AM) hybrid hydrogels expanded, and further adsorption was driven by the osmotic pressure resulting from the concentration difference of Cu^{2+} and Pb^{2+}. The grid size cannot unconditionally increase, because of the stretching limit of P(AA−AM) chain segments; therefore, the adsorption reached saturation (the maximum capacities of monolayer adsorption) when the osmotic pressure resulting from Cu^{2+} and Pb^{2+} in solution was balanced against the stress from the elastic shrinkage of the P(AA−AM) chain segments.

The results from the Freundlich isotherms indicate that the n_F values of sample 5 toward Pb^{2+} were 1.12, 1.14, and 1.19 at 293, 303, and 313 K, respectively, and those of sample 5 toward Cu^{2+} were 1.07, 1.08, and 1.11 at 293, 303, and 313 K, respectively. All of these values are higher than 1, implying the favorable adsorption of sample 5 toward Pb^{2+} and Cu^{2+}.[45]

4. CONCLUSIONS

Novel covalently cross-linked ATP/P(AA−AM) hybrid hydrogels with excellent mechanical stability were prepared by inverse suspension polymerization with non-neutralized AA as the comonomer through the pre-emulsification process. In this process, MF-ATP nanorods were used directly as the sole cross-linker, in the form of an aqueous dispersion without separation. The ATP/P(AA−AM) hybrid hydrogel prepared with a MF-ATP nanorod/comonomer feed ratio of 1:5 with a comonomer utilization (UC) of 96% was optimized to be used as the adsorbent for heavy-metal ions.

The ATP/P(AA−AM) hybrid hydrogels exhibited better adsorption selectivity toward toxic heavy-metal ions such as Pb^{2+} and Cu^{2+}, with equilibrium adsorption capacities of 34.98 and 32.60 mg/g, respectively, in pH 5.0 medium within 9 h. In addition, the adsorbed heavy-metal ions could be desorbed completely with 0.20 mol/L HCl aqueous solution with 100 min, suggesting their excellent reusability. Therefore, ATP/P(AA−AM) hybrid hydrogels are expected to be used as low-cost and effective adsorbents for the removal and recovery of toxic heavy-metal ions from wastewater.

■ ASSOCIATED CONTENT

Ⓢ Supporting Information

Physical appearance of the ATP/P(AA−AM) hybrid hydrogels, kinetics and isotherm models of the adsorption performance of the ATP/P(AA−AM) hybrid hydrogel sample 5 toward Pb^{2+} or Cu^{2+} ions. This material is available free of charge via the Internet at http://pubs.acs.org.

■ AUTHOR INFORMATION

Corresponding Author

*Tel./Fax: 86 0931 8912582. E-mail: pliu@lzu.edu.cn.

Notes

The authors declare no competing financial interest.

■ REFERENCES

(1) *Water Quality for Ecosystem and Human Health*, 2nd ed.; UNEP GEMS/Water Programme: Burlington, Ontario, Canada, 2008.

(2) Gatica, J. M.; Vidal, H. Non-Cordierite Clay-Based Structured Materials for Environmental Applications. *J. Hazard. Mater.* **2010**, *181*, 9−18.

(3) Hua, M.; Zhang, S. J.; Pan, B. C.; Zhang, W. M.; Lv, L.; Zhang, Q. X. Heavy Metal Removal from Water/Wastewater by Nanosized Metaloxides: A Review. *J. Hazard. Mater.* **2012**, *211*, 317−331.

(4) Pan, B. J.; Pan, B. C.; Zhang, W. M.; Lv, L.; Zhang, Q. X.; Zheng, S. R. Development of Polymeric and Polymer-Based Hybrid Adsorbents for Pollutants Removal from Water. *Chem. Eng. J.* **2009**, *151*, 19−29.

(5) Bhatnagar, A.; Sillanpaa, M. Utilization of Agro-Industrial and Municipal Waste Materials as Potential Adsorbents for Water Treatment—A Review. *Chem. Eng. J.* **2010**, *157*, 277−296.

(6) Jing, G. H.; Wang, L.; Yu, H. J.; Amer, W. A.; Zhang, L. Recent Progress on Study of Hybrid Hydrogels for Water Treatment. *Colloids Surf. A: Physicochem. Eng. Aspects* **2013**, *416*, 86−94.

(7) Natkanski, P.; Kustrowski, P.; Bialas, A.; Piwowarska, Z.; Michalik, M. Controlled Swelling and Adsorption Properties of Polyacrylate/Montmorillonite Composites. *Mater. Chem. Phys.* **2012**, *136*, 1109−1115.

(8) Urbano, B.; Rivas, B. L. Poly(sodium 4-styrene sulfonate) and Poly(2-acrylamido glycolic acid) Polymer−Clay Ion Exchange Resins with Enhanced Mechanical Properties and Metal Ion Retention. *Polym. Int.* **2012**, *61*, 23−29.

(9) Natkanski, P.; Kustrowski, P. Influence of Crosslinking Degree on Cu(II) and Fe(III) Adsorption Capacity of Hydrogel/Montmorillonite Composites. *Polimery* **2013**, *58*, 512−518.

(10) Guclu, G.; Al, E.; Emik, S.; Iyim, T. B.; Ozgumus, S.; Ozyurek, M. Removal of Cu^{2+} and Pb^{2+} Ions from Aqueous Solutions by Starch-graft-Acrylic Acid/Montmorillonite Superabsorbent Nanocomposite Hydrogels. *Polym. Bull.* **2010**, *65*, 333−346.

(11) Zheng, Y. A.; Wang, A. Q. Preparation and Ammonium Adsorption Properties of Biotite-Based Hydrogel Composites. *Ind. Eng. Chem. Res.* **2010**, *49*, 6034−6041.

(12) Zheng, Y. A.; Wang, A. Q. Evaluation of Ammonium Removal Using a Chitosan-*g*-Poly(acrylic acid)/Rectorite Hydrogel Composite. *J. Hazard. Mater.* **2009**, *171*, 671−677.
(13) Shawky, H. A.; El-Aassar, A. H. M.; Abo-Zeid, D. E. Chitosan/Carbon Nanotube Composite Beads: Preparation, Characterization, and Cost Evaluation for Mercury Removal from Wastewater of Some Industrial Cities in Egypt. *J. Appl. Polym. Sci.* **2012**, *125*, E93−E101.
(14) Ozgumus, S.; Gok, M. K.; Bal, A.; Guclu, G. Study on Novel Exfoliated Polyampholyte Nanocomposite Hydrogels Based on Acrylic Monomers and Mg−Al−Cl Layered Double Hydroxide: Synthesis and Characterization. *Chem. Eng. J.* **2013**, *223*, 277−286.
(15) Liu, Y.; Wang, W. B.; Jin, Y. L.; Wang, A. Q. Adsorption Behavior of Methylene Blue from Aqueous Solution by the Hydrogel Composites Based on Attapulgite. *Sep. Purif. Technol.* **2011**, *46*, 858−868.
(16) Alaran, M.; Emik, S.; Guclu, G.; Iyim, T. B.; Ozgumus, S. Removal of Acidic Dye from Aqueous Solutions Using Poly-(DMAEMA−AMPS−HEMA) Terpolymer/MMT Nanocomposite Hydrogels. *Polym. Bull.* **2009**, *63*, 159−171.
(17) Kaplan, M.; Kasgoz, H. Hydrogel Nanocomposite Sorbents for Removal of Basic Dyes. *Polym. Bull.* **2011**, *67*, 1153−1158.
(18) Li, P.; Siddaramaiah; Kim, N. H.; Yoo, G. H.; Lee, J. H. Poly(acrylamide/laponite) Nanocomposite Hydrogels: Swelling and Cationic Dye Adsorption Properties. *J. Appl. Polym. Sci.* **2009**, *111*, 1786−1798.
(19) Zhang, X. J.; Zheng, S. J.; Lin, Z. D.; Zhang, J. J. Removal of Basic Fuchsin Dye by Adsorption onto Polyacrylamide/Laponite Nanocomposite Hydrogels. *Synth. React. Inorg., Met.-Org., Nano-Met. Chem.* **2012**, *42*, 1273−1277.
(20) Mahdavinia, G. R.; Massoudi, A.; Baghban, A.; Massoumi, B. Novel Carrageenan-Based Hydrogel Nanocomposites Containing Laponite RD and Their Application to Remove Cationic Dye. *Iran Polym. J.* **2012**, *21*, 609−619.
(21) Li, S. F.; Liu, X. L.; Huang, W. D.; Li, W.; Xia, X. Y.; Yan, S. L.; Yu, J. Y. Magnetically Assisted Removal and Separation of Cationic Dyes from Aqueous Solution by Magnetic Nanocomposite Hydrogels. *Polym. Adv. Technol.* **2011**, *22*, 2439−2447.
(22) Chen, T. Y.; Cao, Z.; Guo, X. L.; Nie, J. J.; Xu, J. T.; Fan, Z. Q.; Du, B. Y. Preparation and Characterization of Thermosensitive Organic−Inorganic Hybrid Microgels with Functional Fe_3O_4 Nanoparticles as Crosslinker. *Polymer* **2011**, *52*, 172−179.
(23) Bhattacharyya, K. G.; Gupta, S. S. Influence of Acid Activation on Adsorption of Ni(II) and Cu(II) on Kaolinite and Montmorillonite: Kinetic and Thermodynamic Study. *Chem. Eng. J.* **2008**, *136*, 1−13.
(24) Sajjadi, S. Particle Formation under Monomer-Starved Conditions in the Semibatch Emulsion Polymerisation of Styrene. Part II. Mathematical Modeling. *Polymer* **2003**, *44*, 223−237.
(25) Slomkowski, S.; Aleman, J. V.; Gilbert, R. G.; Hess, M.; Horie, K.; Jones, R. G.; Kubisa, P.; Meisel, I.; Mormann, W.; Penczek, S.; Stepto, R. F. T. Terminology of Polymers and Polymerization Processes in Dispersed Systems (IUPAC Recommendations 2011). *Pure Appl. Chem.* **2011**, *83*, 2229−2259.
(26) Das, M. Stimulus-Responsive Microgels: Design, Properties and Applications. Ph.D. Thesis, University of Toronto, Toronto, Canada, 2008.
(27) Nebot, V. J.; Armengol, J.; Smets, J.; Prieto, S. F.; Escuder, B.; Miravet, J. F. Molecular Hydrogels from Bolaform Amino Acid Derivatives: A Structure−Properties Study Based on the Thermodynamics of Gel Solubilization. *Chemistry* **2012**, *18*, 4063−4072.
(28) Kitano, H.; Takaha, K.; Gemmei-Ide, M. Raman Spectroscopic Study of the Structure of Water in Aqueous Solutions of Amphoteric Polymers. *Phys. Chem. Chem. Phys.* **2006**, *8*, 1178−1185.
(29) Joachimiak, A.; Halamus, T.; Wojciechowski, P.; Ulanski, J. Structure of Hydrogels Based on Lyotropic Phases of Cellulose Derivative as Studied by Raman Spectroscopy. *Macromol. Chem. Phys.* **2005**, *206*, 59−65.
(30) Myung, D.; Waters, D.; Wiseman, M.; Duhamel, P.; Noolandi, J.; Ta, C. N.; Frank, C. W. Progress in the Development of Interpenetrating Polymer Network Hydrogels. *Polym. Adv. Technol.* **2008**, *19*, 647−657.
(31) Karadag, E.; Uzum, O. B.; Saraydin, D. Swelling Equilibria and Dye Adsorption Studies of Chemically Crosslinked Superabsorbent Acrylamide/Maleic Acid Hydrogels. *Eur. Polym. J.* **2002**, *38*, 2133−2141.
(32) Lu, H.; Shen, H.; Song, Z.; Shing, K. S.; Tao, W.; Nutt, S. Rod-Like Silicate-Epoxy Nanocomposites. *Macromol. Rapid Commun.* **2005**, *26*, 1445−1450.
(33) Chen, Q.; Udomsangpetch, C.; Shen, S. C.; Liu, Y. C.; Chen, Z.; Zeng, X. T. The Effect of AlOOH Boehmite Nanorods on Mechanical Property of Hybrid Composite Coatings. *Thin Solid Films* **2009**, *517*, 4871−4874.
(34) Nathanael, A. J.; Mangalaraj, D.; Chen, P. C.; Ponpandian, N. Enhanced Mechanical Strength of Hydroxyapatite Nanorods Reinforced with Polyethylene. *J. Nanopart. Res.* **2011**, *13*, 1841−1853.
(35) Ljungberg, N.; Cavaille, J. Y.; Heux, L. Nanocomposites of Isotactic Polypropylene Reinforced with Rod-Like Cellulose Whiskers. *Polymer* **2006**, *47*, 6285−6292.
(36) Wang, Y.; Zeng, L.; Ren, X.; Song, H.; Wang, A. Removal of Methyl Violet from Aqueous Solutions Using Poly(acrylic acid-*co*-acrylamide)/Attapulgite Composite. *J. Environ. Sci. (China)* **2010**, *22*, 7−14.
(37) He, Q.; Hu, Z.; Jiang, Y.; Chang, X. J.; Tu, Z. F.; Zhang, L. N. Preconcentration of Cu(II), Fe(III) and Pb(II) with 2-((2-Aminoethylamino)methyl)phenol-Functionalized Activated Carbon Followed by ICP-OES Determination. *J. Hazard. Mater.* **2010**, *175*, 710−714.
(38) Shiratori, S. S.; Rubner, M. F. pH-Dependent Thickness Behavior of Sequentially Adsorbed Layers of Weak Polyelectrolytes. *Macromolecules* **2000**, *33*, 4213−4219.
(39) Chen, H.; Wang, A. Adsorption Characteristics of Cu(II) from Aqueous Solution onto Poly(acrylamide)/Attapulgite Composite. *J. Hazard. Mater.* **2009**, *165*, 223−231.
(40) Zhou, L. M.; Liu, Z. R.; Liu, J. H.; Huang, Q. W. Adsorption of Hg(II) from Aqueous Solution by Ethylenediamine-Modified Magnetic Crosslinking Chitosan Microspheres. *Desalination* **2010**, *258*, 41−47.
(41) Wan Ngah, W. S.; Fatinathan, S. Adsorption Characterization of Pb(II) and Cu(II) Ions onto Chitosan-Tripolyphosphate Beads: Kinetic, Equilibrium and Thermodynamic Studies. *J. Environ. Manage.* **2010**, *91*, 958−969.
(42) Chen, J. J.; Ahmad, A. L.; Ooi, B. S. Poly(*N*-isopropylacrylamide-*co*-acrylic acid) Hydrogels for Copper Ion Adsorption: Equilibrium Isotherms, Kinetic and Thermodynamic Studies. *J. Environ. Chem. Eng.* **2013**, *1*, 339−348.
(43) Liu, Y. Some Consideration on the Langmuir Isotherm Equation. *Colloids Surf. A: Physicochem. Eng. Aspects* **2006**, *274*, 34−36.
(44) Taleb, M. F. A.; Mahmoud, G. A.; Elsigeny, S. M.; Hegazy, E. A. Adsorption and Desorption of Phosphate and Nitrate Ions Using Quaternary (Polypropylene-*g*-*N*,*N*-Dimethylamino Ethylmethacrylate) Graft Copolymer. *J. Hazard. Mater.* **2008**, *159*, 372−379.
(45) Fu, F.; Chen, R.; Xiong, Y. Comparative Investigation of *N*,*N*′-Bis-(dithiocarboxy)piperazine and Diethyldithiocarbamate as Precipitants for Ni(II) in Simulated Wastewater. *J. Hazard. Mater.* **2007**, *142*, 437−442.